



Study of Novel Fe-Based Amorphous/Nanocrystalline Soft Magnetic Powder Cores with NiCuZnFe₂O₄ Coating Layer

Chaohan Zhang¹ · Pingjun Tao¹ · Kunsen Zhu¹ · Yugan Chen¹ · Weijan Zhang¹ · Yuanzheng Yang¹

Received: 16 January 2021 / Accepted: 15 May 2021 / Published online: 2 June 2021
© The Author(s), under exclusive licence to Springer Science+Business Media, LLC, part of Springer Nature 2021

Abstract

The FeSiBCuNb amorphous powder prepared by the ball mill crushing was used as the raw material, and the FeSiBCuNb/NiCuZnFe₂O₄ core–shell structure was prepared by chemical coprecipitation. The soft magnetic powder cores (SMPCs) were then produced from the mixture of the qualified powders with 1 wt% epoxy resin as bonding materials by cold pressing under a compact pressure of 1600 MPa. The evolution of the high-frequency properties for the SMPCs with respect to the annealing temperature was systematically studied. The results show that the prepared NiCuZnFe₂O₄ were evenly coated on the surface of FeSiBCuNb amorphous powder, forming a fine insulating layer. After annealing at the optimal temperature, the SMPCs exhibit excellent magnetic properties: high effective permeability of 80.6 with high-frequency stability up to 2000 kHz; low core loss of 78.18 W/kg at 100 kHz for B_m = 0.1 T, which effectively reduces the high-frequency loss of the SMPCs. The research results are of great significance for the development and performance optimization of the amorphous/nanocrystalline SMPCs.

Keywords FeSiBCuNb amorphous · Soft magnetic powder core · NiCuZn ferrite · Chemical coprecipitation · Effective permeability

1 Introduction

With the continuous development of technology, magnetic materials are widely used in electronic technology and other fields of science and technology [1, 2]. Magnetic material is a kind of functional material with a wide range of uses. Its unique magnetic properties have attracted extensive research [3, 4]. Among them, Fe-based amorphous/nanocrystalline alloys are excellent soft magnetic materials with excellent soft magnetic properties and thermal stability [5]. However, under high-frequency alternating current, skin effect will lead to low permeability and high loss, limiting its application in the high-frequency range [6]. Electronic products are developing toward miniaturization and high frequency with the development of electronic technology, which requires soft magnetic materials to have good frequency stability,

high permeability, high saturation susceptibility, and low iron loss at high frequency. Therefore, it is urgent to develop soft magnetic materials suitable for high frequency [7–9].

Magnetic powder cores (MPCs), a new type of composite magnetic material obtained from magnetic alloy powder by an insulation coating and pressing, are widely used in transformer, DC converter, electronic system, choke, and other fields [10, 11]. Compared with the traditional MPCs including the FeSi, High-flux (FeNi), Sendust (FeSiAl), and FeNiMo powder cores, Fe-based amorphous SMPCs show excellent comprehensive magnetic properties of higher saturation magnetization, higher permeability, and relatively lower core loss at the high-frequency application, and have attracted lots of attention [12, 13]. Insulation coating is a rather important step in the preparation of MPCs [14, 15]. In this key field, researchers have researched and developed methods such as organic coating, inorganic coating and organic–inorganic composite coating [16–18]. Common organic insulating coating agents include epoxy resin, phenolic resin, silicone resin, polypropylene silicone resin, etc. [19]. Although the organic coating has good bonding properties, its poor heat resistance limits the heat treatment temperature of the MPCs [20]. Inorganic coating agents are mainly oxides with high resistivity,

✉ Chaohan Zhang
sphericalcheung@163.com

Pingjun Tao
pjtao@gdut.edu.cn

¹ School of Materials and Energy, Guangdong University of Technology, Guangdong 510006, Guangzhou, China

including SiO_2 [21], Al_2O_3 [22], MgO [23], etc. Although they have good heat resistance and poor adhesion, they are prone to cracking during compression [24]. Since most of its insulating materials are non-magnetic materials, the magnetic powder core's properties are greatly reduced [25, 26]. Ferrite is an ideal electrical insulation coating for soft magnetic composites due to its unique properties such as high resistivity and low eddy current loss [27]. Simultaneously, because ferrite is a soft magnetic material, compared with non-magnetic material coating, the composite magnetic powder core prepared by ferrite coating has more excellent magnetic properties and has become a research hotspot in recent years [15].

At present, the research on ferrite coating mainly focuses on MnZn ferrite [28] and NiZn Ferrite [29]. Among them, NiCuZn ferrite is a high-quality material for preparing a high-frequency magnetic powder core insulation layer due to its low sintering temperature, high resistivity, good temperature stability, and good high-frequency characteristics [30]. In this experiment, $\text{Fe}_{76.8}\text{Si}_{10.5}\text{B}_9\text{Cu}_{0.7}\text{Nb}_3$ amorphous strip was prepared by the single roller method, and then the amorphous powder was obtained by ball milling. Then, a uniform $\text{Ni}_{0.4}\text{Cu}_{0.2}\text{Zn}_{0.4}\text{Fe}_2\text{O}_4$ insulating layer was prepared on the surface of amorphous powder by chemical coprecipitation method. Finally, the amorphous/nanocrystalline SMPCs was obtained by cold pressing and heat treatment. The influence of heat treatment temperature on the properties of $\text{FeSiBCuNb/NiCuZnFe}_2\text{O}_4$ SMPCs was discussed systematically. It is hoped that can provide some new ideas for the preparation of new high-performance nanocrystalline SMPCs and the optimization of the insulating layer and to expand the application of the amorphous/nanocrystalline SMPCs in the high-frequency range.

2 Experiments

2.1 Preparation of $\text{Fe}_{76.8}\text{Si}_{10.5}\text{B}_9\text{Cu}_{0.7}\text{Nb}_3$ Amorphous Powder

$\text{Fe}_{76.8}\text{Si}_{10.5}\text{B}_9\text{Cu}_{0.7}\text{Nb}_3$ alloy ingot was obtained by melting Fe (99.9 wt%), Cu (99.9 wt%), Si (99.8 wt%), Nb (99.6 wt%), and Fe-B (17.51 wt% B) in WK-IIa non-consumable vacuum arc furnace for 4–6 times. The prepared master alloy ingot was placed in the NMS-II type induction melt rapid quenching ribbon spinning machine. The amorphous ribbons were prepared by a single-roll spinning ribbon method under a high-purity Ar atmosphere. Subsequently, the prepared amorphous strip was placed in an NBD-O1200 tube furnace for embrittlement annealing at 330 °C for 1 h. The embrittled ribbons were crushed by ball mill of YXQM-4L planetary ball mill. The ball-to-material ratio was 10:1, the speed was 160 r/min, and the grinding time was 2 h. In the process of ball milling, proper amount of ethanol was added to wet grind to prevent oxidation of magnetic powder. The powders after ball milling were placed in a vacuum drying oven, dried at 50 °C for 1 h, and sieved to obtain the desired amorphous powders.

2.2 Preparation of $\text{Ni}_{0.4}\text{Cu}_{0.2}\text{Zn}_{0.4}\text{Fe}_2\text{O}_4$ Ferrite Insulating Layer

In this experiment, $\text{Ni}_{0.4}\text{Cu}_{0.2}\text{Zn}_{0.4}\text{Fe}_2\text{O}_4$ insulating layer was coated on the surface of $\text{Fe}_{76.8}\text{Si}_{10.5}\text{B}_9\text{Cu}_{0.7}\text{Nb}_3$ amorphous powder by chemical coprecipitation method (the coating content was 5 wt%). The process is shown in Fig. 1. Firstly, the prepared $\text{Ni}(\text{NO}_3)_2 \cdot 6\text{H}_2\text{O}$, $\text{Cu}(\text{NO}_3)_2 \cdot 3\text{H}_2\text{O}$,

Fig. 1 Schematic illustration of $\text{NiCuZnFe}_2\text{O}_4$ coating prepared by chemical coprecipitation



Zn(CH₃COO)₂·2H₂O, Fe(NO₃)₂·9H₂O metal salt, and 3 wt% polyethylene glycol (PEG) were dissolved in 50 ml deionized water by magnetic stirring. The ultrasonically treated amorphous powders were added to it, NaOH solution was added dropwise as a precipitant to adjust the pH to 8–10, and mechanical stirring was maintained at 70 °C in a water bath for 60 min to deposit the NiCuZn ferrite precursor on the surface of the amorphous powder. Then, let it stand for 24 h. The coated powder was washed with deionized water 4–5 times and then dried in a vacuum drying oven at 60 °C.

2.3 Preparation of Amorphous/Nanocrystalline SMPCs

Pour the coated amorphous powder into an agate mortar, add 0.5wt% of KH550 silane coupling agent and a small amount of acetone, 1 wt% epoxy resin was used as curing agent, and continuously grind until the acetone volatilizes to make it thoroughly mixed. Subsequently, 0.5 wt% stearic acid was added as a mold release agent, and cold-pressed under a pressure of 1600 MPa to obtain an amorphous SMPCs with a size of $\Phi 18$ mm \times $\Phi 10$ mm. Finally, the SMPCs were annealed at 500 °C, 550 °C, 600 °C, 650 °C, and 700 °C for 1 h, and nitrogen was used as protective gas. In order to release the internal stress generated in the pressing process, and at the same time make the amorphous powder nanocrystallized.

2.4 Characterization

Phase identification of the powders was performed using X-ray diffraction (XRD, D/Max-IVA, Japan). The morphologies of powder and as-coated powder were examined by scanning electron microscopy (SEM, S-3400 N, Japan) equipped with an energy-dispersive X-ray spectroscopy (EDS). The core loss was measured by the soft magnetic material dynamic measuring instrument FE-2100SA at the frequency ranging from 10 to 100 kHz. The WK 3260B precision magnetic element analyzer was used to measure the SMPCs inductance L (1 ~ 2000 kHz), quality factor Q (1 ~ 2000 kHz), and DC-bias performance (100 kHz, 0 ~ 100 Oe). The effective permeability μ_e of the SMPCs was calculated by the following equation:

$$\mu_e = \frac{LL_e}{\mu_0 N^2 A_e} \quad (1)$$

where L , A_e , and L_e are the inductance, the cross-section area, and the mean flux density path length of the ring sample cores, respectively. N is the total number of coil turns. μ_0 is the permeability of vacuum and it is $4\pi \times 10^{-7}$ H/m.

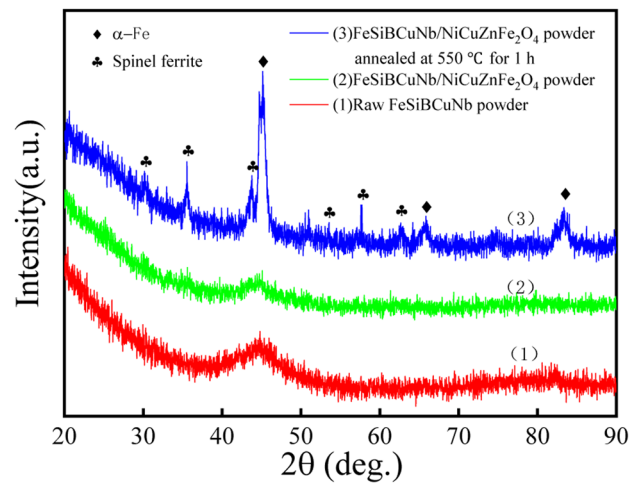


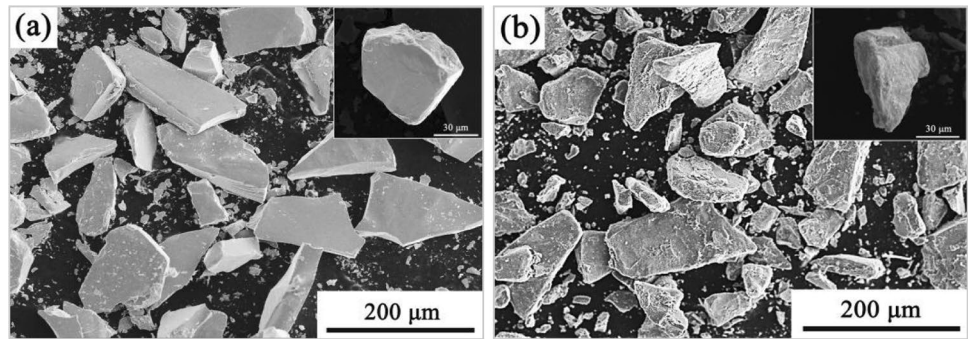
Fig. 2 XRD patterns of original FeSiBCuNb powder, chemically precipitated FeSiBCuNb powder, and FeSiBCuNb/NiCuZnFe₂O₄ powder annealed at 550 °C for 1 h

3 Results and Discussion

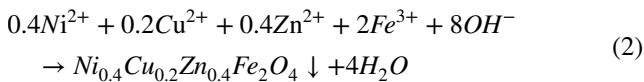
Figure 2 shows the XRD patterns of FeSiBCuNb powder before and after insulation coating and after heat treatment. It can be seen from the figure that there is no sharp diffraction peak of crystal phase in the XRD diffraction spectrum of the original FeSiBCuNb powder, but only a diffuse halo pattern peak near $2\theta = 45^\circ$, indicating that it is a completely amorphous structure. The XRD diffraction spectrum of FeSiBCuNb powder after chemical coprecipitation insulation treatment also shows no apparent peaks, indicating that NiCuZn ferrite precursor deposited on the surface of FeSiBCuNb powder is relatively small or the crystallinity is not high at room temperature. After annealing at 550 °C for 1 h, the XRD diffraction spectrum of FeSiBCuNb/NiCuZnFe₂O₄ powder shows prominent ferrite spinel characteristic peaks, indicating that a coating layer of NiCuZn ferrite with higher crystallinity was formed. The XRD diffraction spectrum also shows sharp diffraction peaks at $2\theta \approx 45^\circ, 65^\circ, 83^\circ$, corresponding to the (110), (200), (211) crystal planes of the α -Fe phase, respectively, indicating that a typical amorphous/nanocrystalline dual-phase structure is formed in the FeSiBCuNb amorphous powder.

To observe the deposition of NiCuZn ferrite, the SEM images of amorphous powder before and after chemical coating are shown in Fig. 3 a and b. The untreated amorphous powder is an irregular polygon with a smooth surface, as shown in Fig. 3a. In contrast, the FeSiBCuNb amorphous powder's surface is uniformly coated with some substance after chemical

Fig. 3 SEM images of FeSiB-CuNb powder before and after coating. (a) Before. (b) After



coprecipitation insulation treatment (Fig. 3b). Representative powder was selected for SEM and EDS analysis to confirm the elemental composition of the surface sediments (Fig. 4a). Figure 4b–d show the EDS spectrum of coated FeSiBCuNb powder. It can be observed that Ni, Cu, and Zn element are uniformly distributed on the surface of the chemically coated flaky powder. The results show that NiCuZn ferrite coating is formed on the surface of FeSiBCuNb amorphous powder after chemical coprecipitation insulation treatment. The reactions in the precipitation process are as follows:

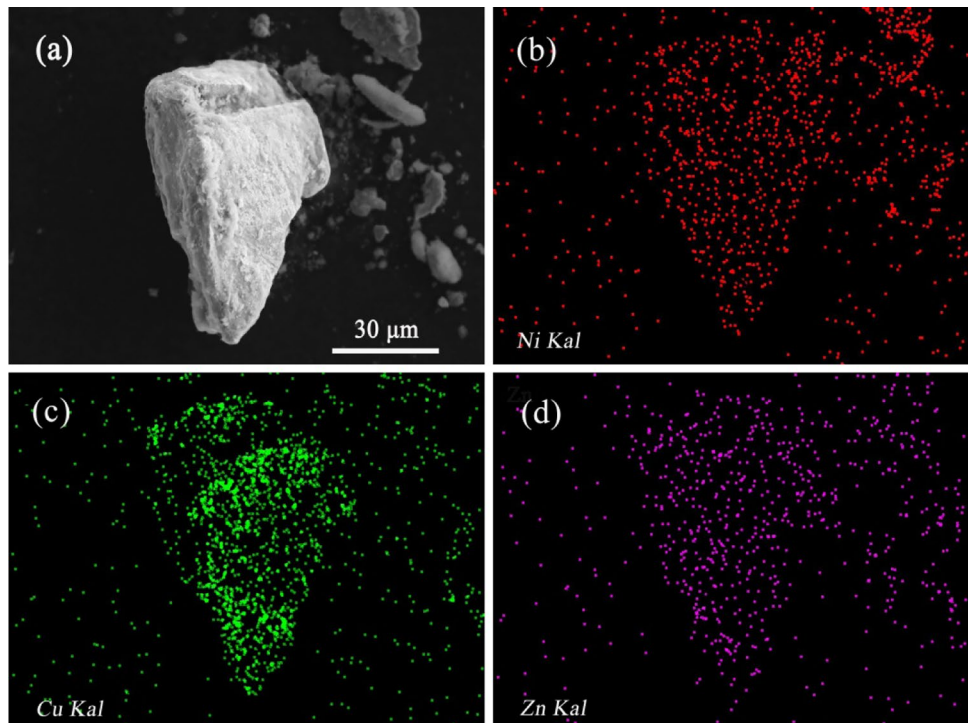


The formation of ferrite in the chemical precipitation process can be explained by the non-uniform nucleation mechanism. With the addition of the precipitant, the ferrite precursor begins to nucleate, and the surface free energy of the

nucleus is extremely high at the initial stage of nucleation. In order to reduce the surface free energy, the crystal nucleus of the precursor product will be adsorbed to the surface of the amorphous powder in the solid solution system. With the continuous progress of the reaction, the ferrite precursor continuously generates non-uniform nucleation on the surface of the amorphous powder, and finally the amorphous powder is completely covered. After the coated powder is heat-treated, the ferrite precursor deposited on the surface forms a ferrite with a spinel structure.

For amorphous/nanocrystalline SMPCs, reasonable annealing temperature can eliminate the internal stress during the pressing process and facilitate the uniform nanocrystalline precipitation in the amorphous matrix to obtain the best soft magnetic properties [31]. Figure 5 shows the frequency dependence of the effective permeability (μ_e) of the SMPCs annealed at 500 to 700 °C. It can be seen that in the frequency range of 1 ~ 2000 kHz, the μ_e of the SMPCs

Fig. 4 SEM images of a typical chemical coated FeSiBCuNb powder (a) and corresponding elemental mapping of (b) Ni, (c) Cu, and (d) Zn



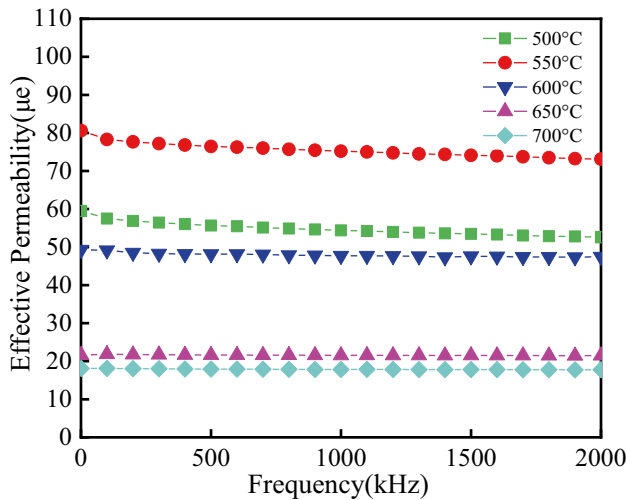


Fig. 5 Frequency dependence of effective permeability of FeSiB-CuNb SMPCs at different annealing temperatures

fluctuate small and has good frequency stability, which indicates that the SMPCs are suitable for components of electronic systems requiring constant permeability in the high-frequency range.

As the annealing temperature increases from 500 to 550 °C, the μ_e of the core increases from 59.5 to 80.6, increasing more than 35%, and the μ_e increases significantly. When the annealing temperature rises to 600 °C, the μ_e decreases to 49.3. When the annealing temperature further increases to 700 °C, the μ_e drops sharply to about 20, and the SMPCs’ performance deteriorates obviously. For the SMPCs annealed at 500 °C, the residual internal stress during cold pressing cannot be eliminated entirely at this temperature, resulting in a decrease of permeability. With the annealing temperature increasing to 550 °C, the residual internal stress of the SMPCs is gradually eliminated, and it can be seen that α -Fe (Si) nanocrystals precipitate in the amorphous powders (Fig. 2), which makes the magnetic soft magnetic properties of the SMPCs better. Simultaneously, the crystallinity of NiCuZn ferrite on the surface of the powder further increases, which also contributes to the increase in magnetic permeability. When the annealing temperature continues to rise, secondary crystallization of the amorphous powder occurs, and a large amount of Fe₂B phase precipitates, resulting in the sharp deterioration of soft magnetic properties and the sharp decline of permeability. In summary, annealing at 550 °C can eliminate the residual stress and obtain uniform distribution of nanocrystals, which is beneficial to the SMPCs to obtain excellent magnetic permeability.

Figure 6 shows the total core loss (P_{cv}) of FeSiBCuNb SMPCs annealed at different temperatures. It can be seen that with the increase of frequency (10–100 kHz) and

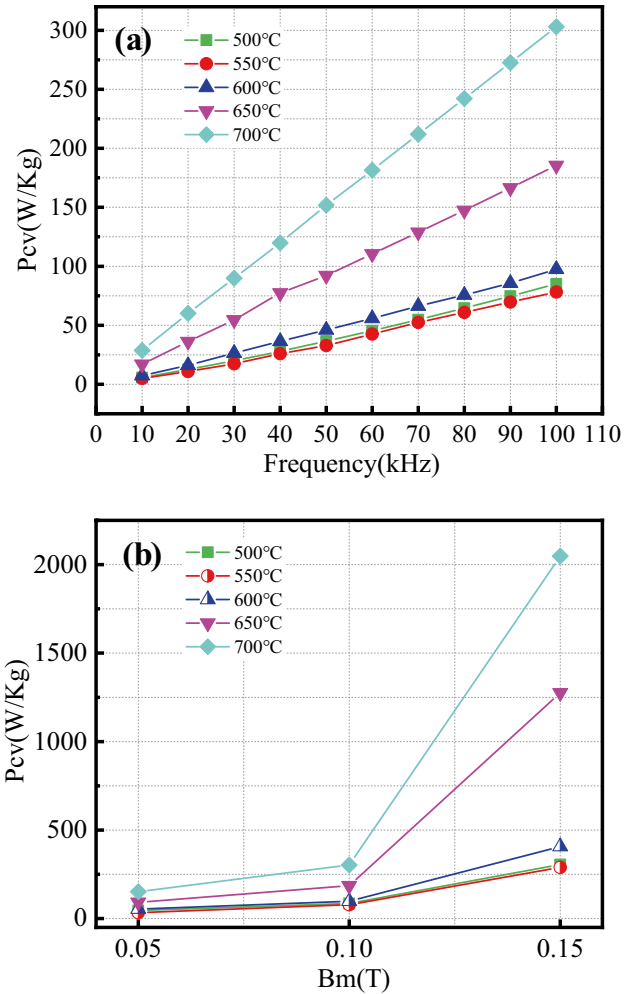


Fig. 6 The total core loss of FeSiBCuNb SMPCs at different annealing temperature. (a) P_{cv} at different frequency ($B_m=0.1$ T). (b) P_{cv} at different magnetic flux density ($f=100$ kHz)

magnetic flux density (0.05–0.15 T), the P_{cv} of all SMPCs samples increased significantly. At $B_m=0.1$ T, $f=100$ kHz, the P_{cv} of the core annealed at 500 °C is 85.11 W/kg. As the annealing temperature increases from 500 to 550 °C, the P_{cv} of the SMPCs gradually decreases, and the lowest value of P_{cv} ($P_{cv}=78.18$ W/kg) is achieved. As the further temperature rises, the P_{cv} gradually increases.

Generally, the loss of magnetic powder core in AC is composed of hysteresis loss (P_h), eddy current loss (P_e), and residual loss (P_r) [32]. The following equation can express the total core loss:

$$P_{CV} = P_h + P_e + P_r = nB^{1.6}f + eB^2f^2 + P_r \tag{3}$$

where n is the hysteresis loss coefficient, B is the flux density, f is the test frequency, and e is the eddy current loss coefficient. Hereinto, the P_r is important only at very low induction levels and very high frequencies and can be

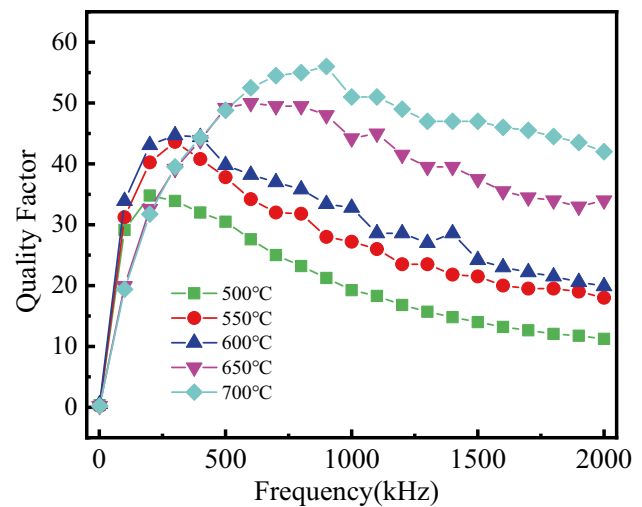
Table 1 Coercivity of FeSiBCuNb SMPCs at different annealing temperatures

Parameters	Annealing temperature (°C)				
	500	550	600	650	700
Coercivity (A/m)	3.62	2.04	4.52	18.42	46.46

ignored in power applications [33]. Thus, only the hysteresis loss and eddy current loss of the SMPCs are discussed here.

The hysteresis loss is usually related to the coercivity (H_c) of the material [34]. When the annealing temperature is low, the residual stress cannot be eliminated entirely, and the H_c is relatively large, which makes the P_h of the SMPCs high. With the increase of temperature, the internal stress of SMPCs processing is gradually eliminated. The formation of nanocrystals reduces the coercivity and then the P_h decreases. Besides, with the increase of temperature, the crystallinity of the NiCuZn ferrite coating layer on the surface of the powder is further increased, which makes the coating effect better and reduces the eddy current loss. It is the reason why the P_{cv} of the SMPCs decrease when the temperature increases from 500 to 550 °C. When the temperature is too high, the growth of nanocrystals and the precipitation of the secondary phase (Fe_2B) increase the coercivity, worsen the magnetic properties, and increase the loss. The numerical change of the coercivity in Table 1 also confirms the above inference. From Eq. (2), the eddy current loss is proportional to the square of f , the core loss is dominated by eddy current loss at high frequencies. The excessively high temperature causes part of the insulating coating on the surface of the powder to fall off, which greatly increases the eddy current loss of the SMPCs. Thus, the loss of the magnetic powder core increases drastically as the temperature increases at high frequencies.

Figure 7 shows the frequency dependence of the quality factor (Q) of the SMPCs annealed at different temperatures. The Q of all SMPCs increases first and then decreases with the increase of frequency. The peak of the frequency characteristic curve of Q reflects the equivalent resistance power loss of the winding in the coil and the conversion of the core power loss mechanism with frequency [16]. At low frequency, the power loss of the magnetic core is low, and the equivalent resistance power loss of the winding is dominant. Therefore, the quality factor of the coil gradually increases with the increase of frequency. When the frequency is high, the power loss increases with the rise in frequency, so the quality factor of magnetic powder core decreases with the rise in frequency. Generally, the value of Q represents the ratio of the stored energy to the loss of the core. With the increase of annealing temperature, the Q of the SMPCs increases gradually. When the annealing temperature is 500 °C, the maximum Q value of the SMPCs is 34.8. When the

**Fig. 7** Frequency dependence of quality factor of FeSiBCuNb SMPCs at different annealing temperatures

annealing temperature increases to 550 °C, the peak value of the Q increases to 43.6. This is because in this temperature range, with the increase of annealing temperature, the core loss decreases gradually, so the Q increases gradually. With the annealing temperature further increasing to 700 °C, the maximum Q of the SMPCs reaches 56. This may be due to the fact that the residual internal stress and some pores impurities are gradually eliminated with the further increase of temperature. At the same time, the precursor of NiCuZn ferrite is almost completely transformed into spinel ferrite with magnetic properties at higher temperature, which enhances the energy storage capacity of the core and increases the Q .

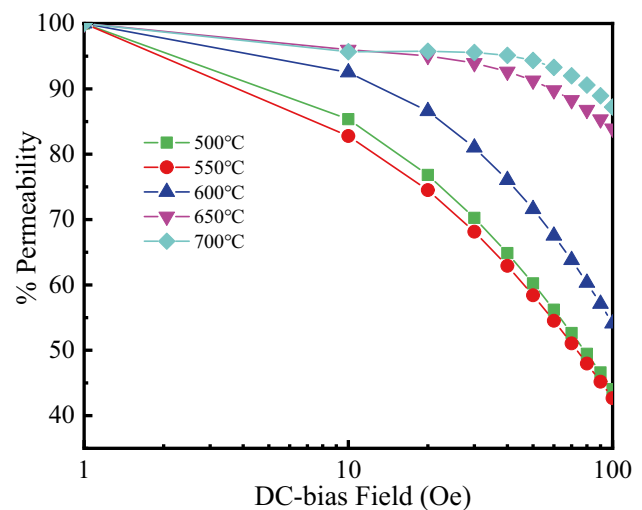
**Fig. 8** The DC-bias field dependence of the permeability for the FeSiBCuNb SMPCs annealed at different temperatures

Figure 8 shows the DC-bias characteristic curves of the FeSiBCuNb SMPCs at different annealing temperatures. The DC-bias characteristic, defined by the percentage of the permeability under the DC-bias field to the permeability without DC-bias field, is reflected in how much the magnetic powder core inductance decreases after the DC-bias field is superimposed [35]. When the applied DC electric field is small, the magnetic induction of the powder core is not saturated, and the inductance attenuation of the core is not obvious. When the applied magnetic field increases, the core inductance decreases significantly [36]. In general, the higher the permeability of the magnetic powder core, the worse its DC-bias characteristics. Conversely, the lower its permeability, the better its DC bias characteristics [37]. The DC-bias characteristic's variation of the FeSiBCuNb SMPCs with the annealing temperature also conforms to the abovementioned law. At 100 Oe, the FeSiBCuNb SMPCs shows 44% DC-bias properties at an annealing temperature of 500 °C. With an annealing temperature of 550 °C, a lower value of 42.6% for percent permeability was obtained due to its higher effective permeability. When the temperature rises to 700 °C, the core's permeability decreases, but the trend of the core being magnetized to saturation is also slowed down, and the DC-bias performance of 87% is obtained. This means that the core has strong DC interference resistance and can be used to deal with the high output current in the power supply.

4 Conclusion

In this paper, the NiCuZnFe₂O₄ insulating layer was prepared on the surface of FeSiBCuNb amorphous powder by chemical coprecipitation method, and FeSiBCuNb/NiCuZnFe₂O₄ nanocrystalline SMPCs were successfully prepared. The effect of annealing temperature on the properties of the core was systematically studied. When annealed at 550 °C for 1 h, the SMPCs exhibit excellent comprehensive magnetic properties, including high permeability of 80.6 with a high-frequency stability up to 2000 kHz, the low core loss of 78.18 W/kg (B_m=0.1 T, 100 kHz), a quality factor of 43.6, 43% DC-bias and lower coercivity 2.04 A/m. This study provides useful enlightenment for the preparation of Fe-based amorphous/nanocrystalline SMPCs and the selection of insulating layer, which can be extended to other Fe-based magnetic powder cores.

Funding This work was supported by National Natural Science Foundation of China (51201038).

References

1. El Yadari, M., Bahmad, L., El Kenz, A., et al.: Monte Carlo study of the double perovskite nano Sr₂VMoO₆[J]. *J. Alloy. Compd.* **579**(23), 86–91 (2013)
2. Masrou, R., Jabar, A., Bahmad, L., et al.: Magnetic properties of mixed integer and half-integer spins in a Blume-Capel model: A Monte Carlo study[J]. *J. Magn. Magn. Mater.* **421**, 76–81 (2017)
3. Mhirech, A., Aouini, S., Alaoui-Ismaili, A., et al.: Bi-layer graphene structure with non-equivalent planes: Magnetic properties study[J]. *Superlattices Microstruct.* **117**, 382–391 (2018)
4. Belhaj, A., Jabar, A., Labrim, H., et al.: Compensation temperature in a dendrimer nano-system with a core-shell structure: Monte Carlo study[J]. *Solid State Commun.* **226**, 54–59 (2016)
5. Azumaa, D., Itoa, N., Ohtaa, M.: Recent progress in Fe-based amorphous and nanocrystalline soft magnetic materials - ScienceDirect[J]. *J. Magn. Magn. Mater.* **501**, 166373 (2020)
6. González-Legarretam, L., Andrejka, F., Marcin, J., et al.: Magneto-impedance effect in nanocrystalline Fe_{73.5}Cu₁Nb₃Si_{13.5}B₉ single-layer and bilayer ribbons [J]. *J. Alloys Comp.* **688**, 94–100 (2016)
7. Hasiak, M., Miglierini, M., Lukiewski, M., et al.: Microstructure, magnetic properties, and applications of co-rich HITPERM-type amorphous alloys[J]. *IEEE Trans. Magn.* **48**(4), 1665–1668 (2012)
8. Krings, A., Boglietti, A., Cavagnino, A., et al.: Soft magnetic material status and trends in electric machines[J]. *IEEE Trans. Industr. Electron.* **64**(3), 2405–2414 (2017)
9. Leary, A.M., Ohodnicki, P.R., Mchenry, M.E.: Soft magnetic materials in high-frequency, high-power conversion applications[J]. *JOM* **64**(7), 772–781 (2012)
10. Otsuka, I., Kadomura, T., Ishiyama, K., et al.: Magnetic Properties of Fe-Based Amorphous Powder Cores With High Magnetic Flux Density[J]. *IEEE Trans. Magn.* **45**(10), 4294–4297 (2009)
11. Wang, X.Y., Lu, C.W., Guo, F., et al.: New Fe-based amorphous compound powder cores with superior DC-bias properties and low loss characteristics[J]. *J. Magn. Magn. Mater.* **324**(18), 2727–2730 (2012)
12. Guo, J.J., Dong, Y.Q., Man, Q.K., et al.: Fabrication of FeSiBPnB amorphous powder cores with high DC-bias and excellent soft magnetic properties [J]. *J. Magn. Magn. Mater.* **401**, 432–435 (2016)
13. Liu, M., Huang, K.Y., Liu, L.T., et al.: Fabrication and magnetic properties of novel Fe-based amorphous powder and corresponding powder cores[J]. *J. Mat. Sci. Mat. Elec.* **29**(7), 6092–6097 (2018)
14. Suzuki, T., Sharma, P., Jiang, L., et al.: Fabrication and properties of under 10 μm sized amorphous powders of high bs soft magnetic alloy for high-frequency applications[J]. *IEEE Trans. Magn.* **99**, 1–5 (2018)
15. Wang, S.M., Yu, Z., Guo, R.D., et al.: Effect of Nano-NiZn ferrite coating on the properties of FeSiCr powder cores[J]. *Journal of Magnetic Materials and Devices* **51**(6), 22–26 (2020)
16. Strečková, M., Fúzer, J., Bureš, R., et al.: Characterization of composite materials based on Fe powder (core) and phenol-formaldehyde resin (shell) modified with nanometer-sized SiO₂[J]. *Bull. Mater. Sci.* **37**(2), 167–177 (2014)
17. Wu, C., Huang, M., Luo, D., et al.: SiO₂ nanoparticles enhanced silicone resin as the matrix for Fe soft magnetic composites with improved magnetic, mechanical and thermal properties[J]. *J. Alloy. Compd.* **741**, 35–43 (2017)
18. Luo, D., Wu, C., Yan, M.: Incorporation of the Fe₃O₄ and SiO₂ nanoparticles in epoxy modified silicone resin as the coating for soft magnetic composites with enhanced performance[J]. *J. Magn. Magn. Mater.* **452**, 5–9 (2018)
19. Wu, S., Sun, A.Z., Zhai, F.Q., et al.: Annealing effects on magnetic properties of silicone-coated iron-based soft magnetic composites[J]. *J. Magn. Magn. Mater.* **324**(5), 818–822 (2012)
20. Xiao, L., Sun, Y., Ding, C., et al.: Annealing effects on magnetic properties and strength of organic-silicon epoxy resin-coated soft magnetic composites[J]. *Proc. Inst. Mech. Eng. C J. Mech. Eng. Sci.* **228**(12), 2049–2058 (2014)

21. Wang, J., Fan, X.A., Wu, Z., et al.: Intergranular insulated Fe/SiO₂ soft magnetic composite for decreased core loss[J]. *Adv Powd Tech*, 1189–1194 (2016)
22. Yaghtin, M., Taghvaei, A.H., Hashemi, B., et al.: Effect of heat treatment on magnetic properties of iron-based soft magnetic composites with Al₂O₃ insulation coating produced by sol-gel method[J]. *J. Alloy. Compd.* **581**, 293–297 (2013)
23. Taghvaei, A.H., Ebrahimi, A., Gheisaril, K., et al.: Analysis of the magnetic losses in iron-based soft magnetic composites with MgO insulation produced by sol-gel method[J]. *J. Magn. Magn. Mater.* **322**(23), 3748–3754 (2010)
24. Luo, F., Fan, X., Luo, Z., et al.: Microstructure, formation mechanism and magnetic properties of Fe_{1.82}Si_{0.18}@Al₂O₃ soft magnetic composites[J]. *J. Magn. Mag. Mat.* **493**, 165744 (2019)
25. Jiang, H., Zhong, W., Wu, X.L., et al.: Direct and alternating current magnetic properties of FeNi particles coated with SiO₂[J]. *J. Alloy. Compd.* **384**, 264–267 (2004)
26. Xie, D.Z., Lin, K.H., Lin, S.T.: Effects of processed parameters on the magnetic performance of a powder magnetic core[J]. *J. Magn. Magn. Mater.* **353**, 34–40 (2014)
27. Li, S.G., Zhang, M.H., Zhan, Z.Z., et al.: Study on novel Fe-based core-shell structured soft magnetic composites with remarkable magnetic enhancement by in-situ coating nano-ZnFe₂O₄ layer[J]. *J. Magn. Magn. Mater.* **500**, 166322 (2020)
28. Wu, S., Sun, A.Z., Xu, W.H., et al.: Iron-based soft magnetic composites with Mn-Zn ferrite nanoparticles coating obtained by sol-gel method[J]. *J. Magn. Magn. Mater.* **324**(22), 3899–3905 (2012)
29. Peng, Y.D., Yi, Y., Li, L.Y., et al.: Iron-based soft magnetic composites with Al₂O₃ insulation coating produced using sol-gel method[J]. *Mater. Des.* **109**, 390–395 (2016)
30. Su, H., Luo, Q., Jing, Y.L., et al.: Effects of calcination temperature and flux doping on the microstructure and magnetic properties of low-temperature-fired NiCuZn ferrites[J]. *J. Magn. Magn. Mater.* **469**, 419–427 (2018)
31. Li, T., Dong, Y.Q., Liu, L., et al.: Novel Fe-based nanocrystalline powder cores with high performance prepared by using industrial materials[J]. *Intermetallics* **102**, 101–105 (2018)
32. Zhou, B., Dong, Y.Q., Liu, L., et al.: The core-shell structured Fe-based amorphous magnetic powder cores with excellent magnetic properties-ScienceDirect[J]. *Adv. Powder Technol.* **30**(8), 1504–1512 (2019)
33. Kollár, P., Biráková, Z., Füzér, J., et al.: Power loss separation in Fe-based composite materials[J]. *J. Magn. Magn. Mater.* **327**(1), 146–150 (2013)
34. Sun, H.B., Wang, C., Wang, J.H., et al.: Fe-based amorphous powder cores with low core loss and high permeability fabricated using the core-shell structured magnetic flaky powders[J]. *J. Magn. Magn. Mater.* **502**, 166548 (2020)
35. Xu, H.P., Wang, R.W., Wei, D., et al.: Crystallization kinetics and magnetic properties of FeSiCr amorphous alloy powder cores[J]. *Journal of Magnetism and Magnetic Materials* **385**, 326–330 (2015).
36. Chang, L., Xie, L., Liu, M., et al.: Novel Fe-based nanocrystalline powder cores with excellent magnetic properties produced using gas-atomized powder[J]. *J. Magn. Magn. Mater.* **452**, 442–446 (2018)
37. Liu, C., Liu, L.G., Yuan, Z.C.: Design and realization of assessment software for DC-bias of transformers[P]. *Proceedings of SPIE - Int. Soc. Opt. Eng.* **8784** (2013)

Publisher's Note Springer Nature remains neutral with regard to jurisdictional claims in published maps and institutional affiliations.